BIOCHEMISTRY
including biophysical chemistry & molecular biology

Article

Lid Opening and Unfolding in Human Pancreatic Lipase at Low pH Revealed by Site-Directed Spin Labeling EPR and FTIR Spectroscopy

Sebastien Ranaldi, Vale#rie Belle, Mireille Woudstra, Jorge Rodriguez, Bruno Guigliarelli, James Sturgis, Frederic Carriere, and Andre Fournel

Biochemistry, **Article ASAP** • DOI: 10.1021/bi801250s

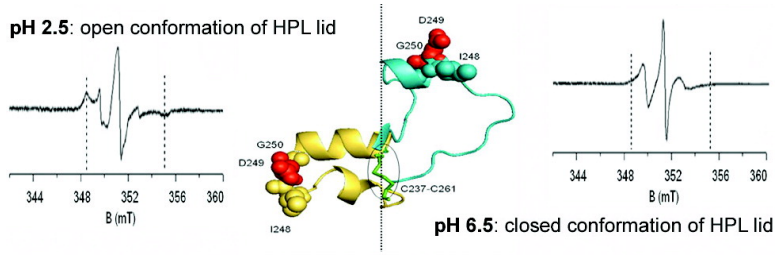

More About This Article

Additional resources and features associated with this article are available within the HTML version:

- Supporting Information
- Access to high resolution figures
- Links to articles and content related to this article
- Copyright permission to reproduce figures and/or text from this article

View the Full Text HTML

Biochemistry is published by the American Chemical Society. 1155 Sixteenth Street N.W., Washington, DC 20036

Lid Opening and Unfolding in Human Pancreatic Lipase at Low pH Revealed by Site-Directed Spin Labeling EPR and FTIR Spectroscopy†

Sebastien Ranaldi,‡ Valérie Belle,‡ Mireille Woudstra,‡ Jorge Rodriguez,§ Bruno Guigliarelli,‡ James Sturgis,|| Frederic Carriere,*,§ and Andre Fournel*,‡

CNRS Laboratoire de Bioénergétique et Ingénierie des Protéines, UPR 9036, Marseille, France, CNRS Laboratoire d'Enzymologie Interfaciale et de Physiologie de la Lipolyse, UPR 9025, Marseille, France, and CNRS Laboratoire d'Ingénierie des Systèmes Membranaires, UPR 9027, Institut de Microbiologie de la Méditerranée, Aix-Marseille Universités, Marseille, France

Received July 2, 2008; Revised Manuscript Received November 16, 2008

ABSTRACT: The structural changes induced in human pancreatic lipase (HPL) by lowering the pH were investigated using a combined approach involving the use of site-directed spin labeling coupled to electron paramagnetic resonance (SDSL-EPR) and Fourier transform infrared (ATR-FTIR) spectroscopy. The secondary structure of HPL observed with ATR-FTIR spectroscopy was found to be stable in the pH range of 3.0−6.5, where HPL remained active. Using a spin-label introduced into the lid of HPL at position 249, a reversible opening of the lid controlling the access to the active site was observed by EPR spectroscopy in the pH range of 3.0−5.0. In the same pH range, some structural changes were also found to occur outside the lid in a peptide stretch located near catalytic aspartate 176, using a spin-label introduced at position 181. Below pH 3.0, ATR-FTIR measurements indicated that HPL had lost most of its secondary structure. At these pH levels, the loss of enzyme activity was irreversible and the ability of HPL to bind to lipid emulsions was abolished. The EPR spectrum of the spin-label introduced at position 181, which was typical of a spin-label having a high mobility, confirmed the drastic structural change undergone by HPL in this particular region. The EPR spectrum of the spin-label at position 249 indicated, however, that the environment of this residue within the lid was not affected at pH 3.0 in comparison with that observed in the pH range of 3.0−5.0. This finding suggests that the disulfide bridge between the hinges of the lid kept the secondary structure of the lid intact, whereas the HPL was completely unfolded.

Pancreatic lipase is the main catalyst of dietary fat lipolysis (*1*). Studies on the three-dimensional structure of human pancreatic lipase (HPL)[1] have shown that this lipase contains a globular N-terminal domain with an α/β-hydrolase fold, an active site with a Ser-His-Asp catalytic triad, an oxyanion hole, and a C-terminal domain which is involved in colipase and lipid binding (*2*−*5*). The active site of HPL is covered by an amphiphilic domain, the so-called lid that can undergo a change in conformation, depending on its environment. The lid was found to be in the closed conformation in the first structure obtained, with no access to the active site (*2*), whereas the presence of amphiphiles (bile salts and phospholipids) and inhibitor in the crystallization mixture induced the opening of the lid and a functional active site was observed (*4*). The lid opening process was recently monitored in solution, using site-directed spin labeling (SDSL) methods coupled to electron paramagnetic resonance (EPR) spectroscopy (*6*). After introduction of a spin-label into the lid, specific EPR spectra were attributed to the closed and open conformations of the HPL lid using factors known to induce lid opening (bile salts, colipase, and E600 lipase inhibitor).

In addition to these conformational changes, catalysis by HPL is characterized by the fact that the enzyme is water soluble, whereas triglycerides, which are its natural substrate, are not. Before the hydrolysis of triglycerides can occur at an oil−water interface, the lipase must first bind to this interface, and the adsorption step is a specific feature of interfacial enzymes (Figure 1). It has been assumed that the lid opening process and the generation of a large hydrophobic surface around the active site of HPL promote the adsorption of the lipase. This point is still a matter of debate, however, since some experiments have suggested that inactive lipases with a closed lid might also be able to bind to lipid−water interfaces (*7*).

When studying enzymes such as lipases, one must bear in mind the fact that the adsorption step can be the limiting step for the apparent enzyme activity. This point should be taken into account when the effects of classical parameters such as the pH, for instance, are studied. This was illustrated

† S.R.'s Ph.D. research was supported by a grant from the French Ministry of Research and Education.

* To whom correspondence should be addressed: IBSM, CNRS, 31 chemin Joseph Aiguier, 13402 Marseille cedex 20, France. Telephone: (33) 4 91 16 45 57. Fax: (33) 4 91 16 45 78. E-mail: carriere@ibsm.cnrs-mrs.fr or fournel@ibsm.cnrs-mrs.fr.

‡ UPR 9036.

§ UPR 9025.

|| UPR 9027.

[1] Abbreviations: DGL, dog gastric lipase; EPI, exocrine pancreatic insufficiency; HPL, human pancreatic lipase; SDSL, site-directed spin labeling; EPR, electron paramagnetic resonance spectroscopy; MTSL, (1-oxyl-2,2,5,5-tetramethyl-Δ^3-pyrroline-3-methyl) methanethiosulfonate; ATR-FTIR, attenuated total reflection Fourier transform infrared spectroscopy.

10.1021/bi801250s CCC: $40.75

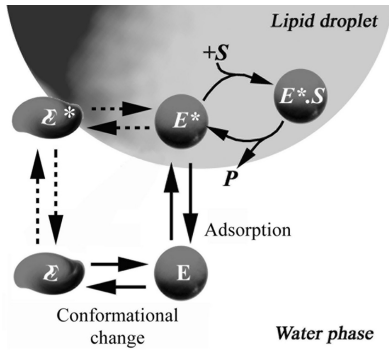

FIGURE 1: Schematic kinetic model of interfacial catalysis by pancreatic lipase. This model shows the three main steps involved in the overall catalytic process: the change in the conformation of the lipase (E) corresponding to the opening of the lid, the lipase adsorption occurring at the lipid−water interface (E*), and the interfacial Michaelis−Menten reaction.

by the characterization of dog gastric lipase (DGL), a lipase with an optimum activity at pH 4.0 on long chain triglycerides (*8*). The three-dimensional (3D) structure of DGL comprises a Ser-His-Asp catalytic triad and an oxyanion hole (*9*), like that of most serine enzymes exhibiting an optimum activity at pH >7.0. The kinetic properties of DGL were therefore not consistent with the ionization properties of histidine (pK_a = 6.5) and the fact that this residue is known to play an important role in the charge relay system involving the catalytic triad and the enhancement of the nucleophilic character of the serine residue. The 3D structure of DGL did not, however, show any specific features at the level of the catalytic triad that might account for the local change in the histidine pK_a and the fact that the optimum activity of DGL occurred at low pH levels. This apparent discrepancy was later resolved when it was established that the DGL adsorption occurring at lipid−water interfaces and hydrophobic surfaces is pH-dependent and that the maximum levels of adsorption, and therefore the maximum rates of activity, occur at low pH values (*10*). Other studies have suggested that lipases might preferentially bind to interfaces at low pH levels. The maximum level of adsorption of porcine pancreatic lipase onto tributyrin emulsions was observed at pH 4.5 in the presence of bile salts and in the absence of colipase (*11*). Under these conditions, the lipase adsorption rate was found to decrease with an increase in pH, and the maximum apparent activity of the lipase was observed at pH 5.5 (*11*). Adding colipase gave more efficient adsorption of the pancreatic lipase on its aggregated substrate at higher pH values, and the maximum apparent activity of the lipase shifted to pH 7.0 (*11*).

Since the overall process of interfacial catalysis involves a conformational change in the lipase lid (Figure 1), the effect of the pH on this particular step should also be taken into account. Using the SDSL-EPR method previously developed for monitoring the HPL lid opening process (*6*), the effects of pH on the pancreatic lipase lid conformation were investigated here for the first time in the absence of any lipid, inhibitor, or detergent. Measurements were performed from pH 6.5 to 2.5. The reason for this choice of pH range was that it includes the physiological range existing in vivo in the gastrointestinal tract. HPL is exposed in vivo to pH values ranging from 5.5 to 6.5 on average in healthy humans (*1, 12, 13*) to values as low as 2.0−3.0 in the small intestine of patients with exocrine pancreatic insufficiency (EPI) (*14, 15*). Local structural changes were observed in the vicinity of the active site using spin-labels introduced either into the lid (at position 249) or at position 181, where a cysteine residue naturally occurs in HPL, while the evolution of the global HPL secondary structure was monitored via performance of ATR-FTIR spectroscopy. The effects of pH on the stability of HPL were also investigated by measuring the residual activity of HPL on tributyrin, as well as by assessing the ability of this lipase to adsorb onto trioctanoin emulsions.

MATERIALS AND METHODS

Production of Recombinant HPL and the HPL Mutant. All the procedures used here have been previously described in detail by Belle et al. (*6*). The cDNA encoding HPL was previously obtained from human placenta mRNA using PCR methods (*16*). A 1411 bp *Bam*HI DNA fragment containing the entire HPL coding region was subcloned into the pGAPZB *Pichia pastoris* transfer vector (Invitrogen) downstream of the GAP constitutive promoter for further expression of HPL from the yeast *P. pastoris*. The HPL C181Y-D249 mutant was constructed using the PCR overlap extension technique as previously described, and this mutant was also produced in *P. pastoris* after its DNA had been inserted into the pGAPZB vector. Wild-type *P. pastoris* strain X-33 was transformed by electroporation using linearized pGAPZB vectors containing either HPL or HPL mutant DNA. Cell cultures were then performed in 1 L Erlenmeyer flasks containing 200 mL of YPD medium without any Zeocin, and the cell growth was stopped after 40 h to limit the proteolysis of the recombinant HPL (or mutant) secreted into the culture medium.

For the purification of HPL and the HPL mutant, 2 L of yeast culture medium was collected and the pure proteins were obtained after a single cation exchange chromatography step on S-Sepharose gel (Pharmacia). The purified lipases were characterized via measurement of their lipase activity, performing SDS−PAGE, N-terminal sequencing, and MALDI-TOF mass spectrometry analysis.

Spin Labeling Procedure. Since free cysteines were observed to be oxidized in the recombinant lipase recovered from *Pichia* culture medium, the recombinant proteins were first reduced with DTT prior to the spin labeling reaction. HPL (8−10 mg/mL) was incubated with a 10-fold molar excess of DTT for 30 min in ice. The excess DTT was then removed by performing gel filtration chromatography on a Superdex 75 column, using 10 mM MES, 150 mM NaCl buffer (pH 6.5). The fractions containing lipase activity were pooled and concentrated using 30 kDa cutoff polyethersulfone ultrafiltration membranes (Vivaspin 2, VivaSciences-Sartorius) to reach a lipase concentration of around 8−10 mg/mL with a minimum loss of protein. The HPL was then labeled with (1-oxyl-2,2,5,5-tetramethyl-Δ3-pyrroline-3-methyl) methanethiosulfonate (MTSL, Toronto Research Chemicals Inc., Toronto, ON) at a molar excess of 10, using a stock MTSL solution at a concentration of 10 mg/mL in acetonitrile. The reaction was carried out for 1 h in ice, under gentle stirring, and a continuous flow of nitrogen was provided to prevent the occurrence of oxidation. The excess MTSL was then removed by performing a second gel filtration chromatography step on a Superdex 75 column,

using 10 mM MES, 150 mM NaCl buffer (pH 6.5). All the fractions were checked by performing EPR spectroscopy, and those giving an EPR spectral shape typical of a labeled protein were pooled and concentrated at around 4 mg of HPL/mL (80 μM), as described above.

Incubation of HPL Samples at Various pH Values. The spin-labeled HPL was incubated at various pH values for various times ranging from 15 to 240 min. The pH values were adjusted by mixing the enzyme solution [100 μM HPL in 10 mM MES and 150 mM NaCl (pH 6.5)] in a 1:1 volume ratio with a 200 mM glycine buffer set at the desired pH. We checked that the glycine buffer used was sufficiently strong to keep the pH of the mixture constant.

Samples of the incubation mixture were taken at various times and used directly to record EPR spectra and to assess the HPL stability by measuring the residual lipase activity, except when the reversibility of the pH effects was probed. In this case, we first increased the pH of the lipase solution to pH 7.5 before measuring the residual lipase activity and performing EPR spectroscopy. A solution of 0.01 N NaOH was used to increase the pH value, and the volume added was sufficiently small (microliters) to keep the concentration of spin-labeled HPL compatible with standard EPR experiments.

Collection of EPR Data. EPR spectra were recorded at 25 °C in a temperature-controlled room using an ESP 300E Bruker spectrometer equipped with an ELEXSYS Super High Sensitivity resonator operating at 9.9 GHz. The spin-labeled HPL mutant concentrations were in the range of 40−80 μM. They were injected into a quartz capillary tube with a useful volume of ~20 μL. The microwave power was set at 10 mW, and the magnetic field modulation frequency and amplitude were 100 kHz and 0.1 mT, respectively.

The spin labeling yield was assessed by comparing the integration of the EPR spectrum of the labeled HPL recorded under nonsaturating conditions with that obtained with a 3-carboxy-proxyl sample at a known concentration.

Residual Lipase Activity Measurements. The residual activity of the HPL was measured using the pHstat technique with a mechanically stirred emulsion of tributyrin (TC4, puriss grade from Fluka) as the substrate (*16*). Using a TTT 80 Radiometer pH-stat (Copenhagen, Denmark), the free fatty acids released by the 1 μL lipase samples were automatically titrated with 0.1 N NaOH at a constant pH value of 7.5. Each reaction was performed in a thermostated vessel (37 °C) containing 0.5 mL of TC4, 14.5 mL of 0.28 mM Tris-HCl buffer, 150 mM NaCl, 1.4 mM $CaCl_2$, 0.5 mM sodium taurodeoxycholate (NaTDC), and colipase in a large excess. Recombinant HPL shows a maximum specific activity of 12500 units/mg under these conditions. The lipolytic activities recorded are expressed here in international units (U). One unit corresponds to 1 μmol of fatty acid released per minute.

Lipase Adsorption Measurements. The interfacial binding of HPL was assayed by mixing the enzyme with a trioctanoin emulsion formed in a pH-stat vial and measuring the amount of lipase remaining in the water phase after the separation of the oil phase. The pH-stat vial was placed on the automatic titrator (TTT 80 Radiometer), and its contents were stirred mechanically for 5 min to produce a fine trioctanoin emulsion and to maintain the pH at the desired level via addition of NaOH or acetic acid. Colipase was added during this 5 min period. HPL was then added to the emulsion. After incubation for 2 min, the content of the pH-stat vial was transferred into a 25 mm × 64 mm centrifuge tube (Beckman ultra-Clear), which was kept on the bench for 1 h to allow a satisfactory phase separation. After a creaming step, a sample (1−2 mL) of the clear aqueous phase was recovered by introducing a 0.8 mm × 40 mm needle equipped with a 5 mL syringe into the bottom of the tube. The amount of lipase present in the aqueous phase was determined by performing an ELISA as previously described (*17*).

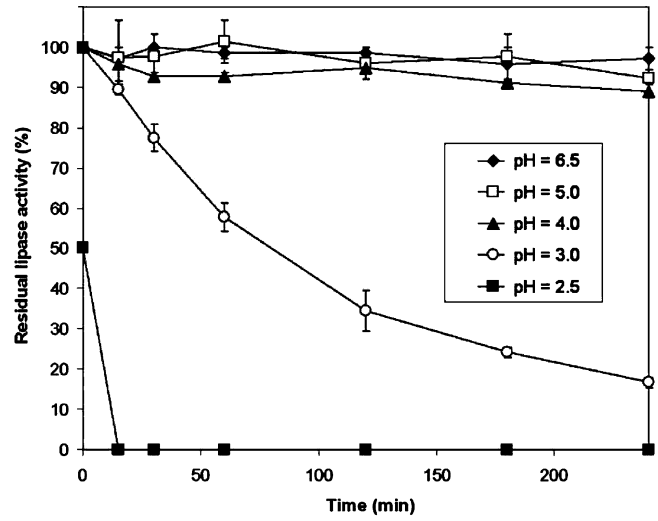

FIGURE 2: pH stability of HPL assessed by performing residual activity measurements. The pH values were adjusted by mixing the enzyme solution [100 μM HPL in 10 mM MES and 150 mM NaCl (pH 6.5)] with a 200 mM glycine buffer set at the required pH, in a 1:1 volume ratio. The final HPL concentration (50 μM) was in the same range as that used for the EPR studies. Samples from the incubation mixture were taken at various times, and the residual activity of HPL was measured at pH 7.5 using the pH-stat technique and expressed as a percentage of the initial activity of HPL stored at pH 7.5. Values are means ± the standard deviation (SD) (n = 3).

Collection of FTIR Data. Attenuated total reflectance Fourier transform infrared (ATR-FTIR) spectra were recorded using a Bruker Equinox 55 spectrometer equipped with a SensIR-DurasamplirII three-reflection diamond ATR crystal. The spectra shown here (Figure 6) are the average of 500 scans with a resolution of 2 cm^{-1}, after subtraction of the spectrum of the buffer. Approximately 5 μL of lipase sample or buffer was transferred to the ATR crystal, and the droplet was covered to prevent evaporation. The lipase concentrations in the samples tested ranged from 4.5 to 7 mg/mL. Data were processed using the dedicated OPUS software program. The ATR to absorption spectrum conversion was performed to compensate for any frequency-dependent path length variations. Spectral deconvolution was performed using Fourier self-deconvolution followed by Gaussian band fitting methods.

RESULTS

Effects of pH on HPL Activity and Adsorption Properties. The stability of HPL at various acidic pH levels was investigated by measuring the residual activity of HPL after several incubation times in a buffer adjusted to a precise pH value (Figure 2). At pH levels ranging from 4.0 to 6.5, the residual activity of HPL remained higher than 90% after incubation for 2 h. At pH 3.0, the residual activity of HPL

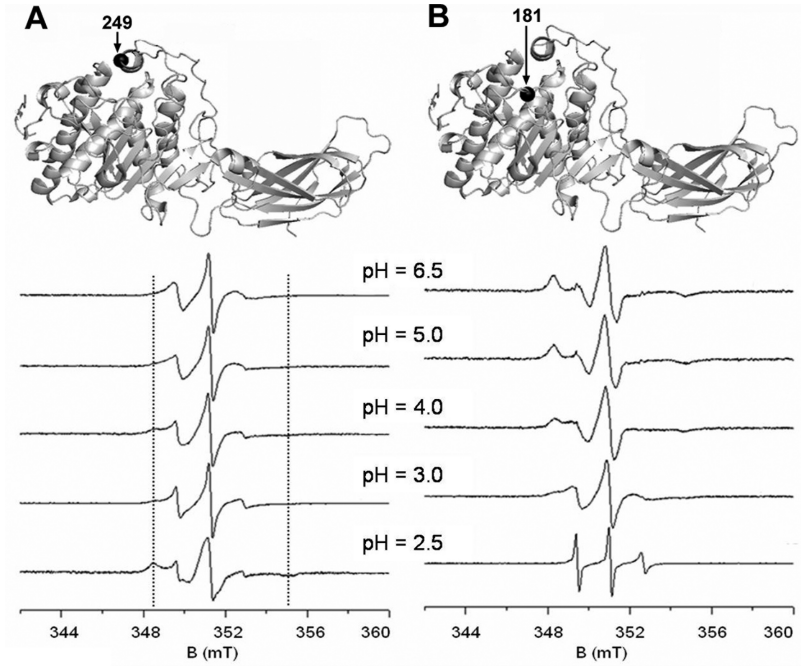

FIGURE 3: EPR spectra of HPL labeled at position 249 (A) and position 181 (B) as a function of pH. The spectra were recorded at 25 °C using an ESP 300E Bruker spectrometer equipped with an ELEXSYS Super High Sensitivity resonator operating at 9.9 GHz. Spin-labeled HPL samples were injected into a quartz capillary tube with a useful volume of ~20 μL, and the enzyme concentration was 50 μM. The amplitude of all the EPR spectra was normalized on the basis of the central line of the spectrum. The dotted lines in panel A give the position of the low- and high-field lines of the slow-motion component of the EPR spectrum.

decreased with time: a 50% decrease in the activity was observed after an incubation time of approximately 80 min. At pH 2.5, no residual activity was detected after an incubation time of 15 min. When the residual activity was measured immediately after the pH of the sample had been adjusted to 2.5, approximately 50% of the activity was already lost. All in all, these results indicate that pH values of $\leq$3.0 have destabilizing effects on HPL, showing slow kinetics at pH 3.0 and faster kinetics (not measurable) at pH 2.5.

HPL adsorption at the water−lipid interface (trioctanoin emulsion) was also measured at various pH values covering the same range. At pH values ranging from 4.0 to 6.5, the proportion of the HPL remaining in the aqueous phase was found to range between 25 and 50% (data not shown), which indicates that a large proportion of the enzyme was adsorbed at the water−lipid interface. At pH values of 2.5 and 3.0, all the HPL was found to be present in the aqueous phase, which indicates that the enzyme had lost its ability to bind to the lipid−water interface at these particular pH values. It is worth noting that the values obtained by performing an ELISA to quantify the HPL present in the water phase were performed after 1 h, which is the time required for the complete phase separation process to occur. The amounts of HPL recovered in the water phase might therefore not reflect the initial conditions.

In addition, the ability of HPL to bind to its cofactor colipase was also tested (data not shown) by performing competition experiments as described in ref *17*. After incubation of HPL at pH 2.5, the HPL−colipase interaction was lost.

The pH value of 3.0 therefore appeared to be a threshold value for most of the functional properties of HPL.

Effects of pH on the EPR Spectra of Spin-Labeled HPL. HPL labeled at two different sites with nitroxide radicals (MTSL) was studied by performing EPR spectroscopy at various pH levels. We first checked that the EPR spectrum of MTSL was not sensitive to pH variations (data not shown). The spin-label was then introduced at position 181 into wild-type HPL, where a cysteine residue naturally occurs. This cysteine, C181, is exposed at the surface of HPL near the active site, but its conformation was apparently not affected by the conformational changes associated with the opening of the lid (*3, 4, 6*). On the other hand, a spin-label grafted onto the lid at position 249 was previously used to monitor the conformational changes occurring in the lid under various experimental conditions (*6*). Among the 23 amino acid residues constituting the lid, residue 249 was chosen because it is not involved in any functional interactions and its side chain is always accessible to solvent, based on the available 3D structural data of HPL. A cysteine residue was introduced into the lid via the D249C mutation, and the C181 residue present in wild-type HPL was replaced with a tyrosine using site-directed mutagenesis methods, to have a single labeling site on the HPL molecule. In this study, the effects of pH on the EPR spectra of the HPL labeled at position 181 or 249 (Figure 3) were monitored. We previously checked that the mutations and chemical modifications of HPL had no effect on the main kinetic properties of the lipase (*6*).

With the spin-label grafted onto the lid (Figure 3A), the EPR spectrum obtained at pH 6.5 exhibited an outer line splitting of 3.2 mT. As the pH decreased, a composite spectrum appeared, with a broad shape component characterized by an outer line splitting of 6.6 mT (see dotted lines), which will here be termed the slow-motion component (for further comments on the motion of the probe, see Discussion). To assess the relative proportion of this slow-motion component, we subtracted the narrow shape component (fast motion of the spin-label with a 3.2 mT outer line splitting) from the composite spectra. The relative proportion of the

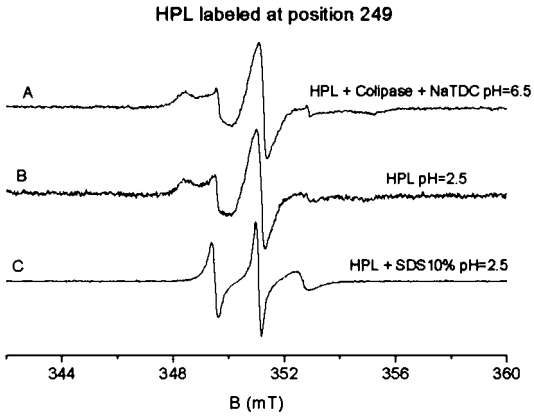

FIGURE 4: Comparison between the EPR spectra of the HPL labeled at position 249 under various conditions: (A) HPL with colipase in a molar excess of 2 and 4 mM NaTDC at pH 6.5, (B) HPL alone at pH 2.5, and (C) HPL after denaturation by 10% SDS at pH 2.5. The amplitude of all the EPR spectra was normalized on the basis of the central line of the spectrum.

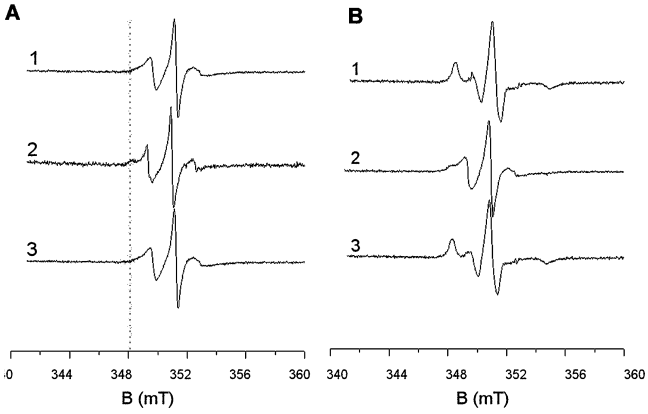

FIGURE 5: Reversible effect of pH on HPL labeled at position 249 (A) and 181 (B): (1) initial spectrum measured at pH 6.5, (2) spectrum measured after the pH had been decreased to pH 3.0 (identical spectra were obtained after various incubation times ranging from 5 to 90 min), and (3) spectrum measured after the pH had been shifted from 3.0 to 6.5 via addition of NaOH to the sample.

slow-motion component was expressed as the ratio I_2/I_1, where I_1 and I_2 are the integrated intensity of the composite spectra and that of the result of the subtraction, respectively.

In the pH range of 3.0−6.5, the relative proportion of the slow-motion component was found to be variable, reaching a maximum value of 50 ± 5% at pH 4.0. At pH 2.5, a jump in the distribution of the two spectral shapes was observed, giving an I_2/I_1 ratio as high as 90 ± 5%. Interestingly, the slow-motion component of the EPR spectrum was identical to that observed at pH 6.5 in the presence of the natural physiological partners of HPL, colipase, and bile salts (Figure 4A,B), which was attributed to HPL being in the open conformation (*6*).

The EPR spectral shape of the spin-label grafted at position 181 (Figure 3B) indicated that the mobility of the label was low at pH 6.5. In our previous study, this low spin-label mobility was attributed to the presence of steric hindrances at this particular location, which is at the bottom of a small surface pocket of the enzyme (*6*). Figure 3B shows that the spectral shape remained unchanged between pH 6.5 and 4.0. A change in the spectral shape was observed at pH 3.0, and more pronounced changes were detected at pH 2.5, where

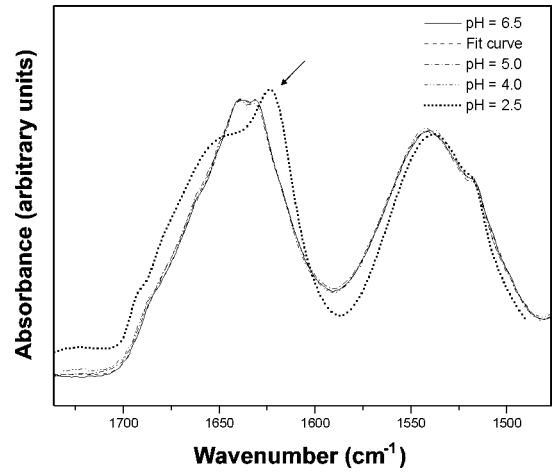

FIGURE 6: FTIR spectrum of HPL in the 1750−1500 cm^{-1} region at various pH values in H_2O medium. The FTIR spectrum of HPL (solid line) is shown after digital subtraction of the buffer spectrum in the region of the amide I and amide II bands. The spectrum shown as a dotted line was obtained by deconvolution of the FTIR spectrum with Gaussian functions. Lipase concentrations in the samples tested ranged from 4.5 to 7 mg/mL.

the EPR spectrum obtained was that typical of a spin-label grafted onto an unfolded or poorly structured protein, while the nitroxide obeyed a fast-motion regime (*18*−*20*). At the lowest pH value tested (2.5), very different spectral shapes were therefore observed between the HPL labeled on the lid (at position 249) and the HPL labeled at position 181. The spectral shape obtained in the former case, corresponding to a low-mobility spin-label, suggests the occurrence of a local folding of the protein, whereas that obtained in the second case suggests a locally unfolded state of HPL. The further treatment with SDS (10%, w/v) of the HPL labeled at position 249 gave an EPR spectral shape typical of a spin-label grafted to a denatured or poorly structured protein (Figure 4C), which was similar to the shape obtained at pH 2.5 with the spin-label at position 181 (Figure 3). The unfolding of HPL is therefore not complete at pH 2.5, where a local structure located around position 249 is still preserved.

Reversibility of the pH-Dependent Effects on the Spin-Labeled HPL. The reversibility of the pH-dependent effects on the spin-labeled HPL at position 249 or 181 was studied by recording EPR spectra at low pH levels (2.5, 3.0, 4.0, and 5.0) followed by an EPR study on the same sample after the pH had been shifted to 6.5. Figure 5 shows the EPR spectra of the HPL labeled at position 249 (panel A) and position 181 (panel B) at the initial pH level of 6.5 (spectra 1), after the pH had been decreased to 3.0 (spectra 2) and after the pH had been increased back to 6.5 (spectra 3). With each spin-labeled HPL and whatever the incubation time tested, the initial EPR spectrum recorded at pH 6.5 was recovered after incubation of the enzyme sample at pH 3.0, 4.0, or 5.0, which indicates that the structural destabilization of the enzyme was reversible down to pH 3.0. When the preincubation pH level was 2.5, the changes in the EPR spectra were found to be irreversible (data not shown). The pH value of 3.0 therefore seems to be a threshold value at which a larger structural destabilization of HPL occurs.

Effects of pH on HPL Studied by FTIR. As SDSL-EPR spectroscopy findings showed that the effects of pH on the structure of HPL seemed to depend on the probe position, FTIR studies were performed on HPL to monitor the effects

Table 1: Positions, Widths, Integrals, and Attribution of the Set of Gaussians Resulting from the Deconvolution of the HPL Amide I Absorption Band Obtained via Performance of ATR-FTIR Spectroscopy

position (cm^{-1})	width	integral	structural component
1624	30.52	1.46	β-strand
1683	21.22	0.35	β-strand
1643	22.06	0.76	α-helix
1657	27.58	0.62	α helix
1665	22.23	0.39	turn
1630	9.22	0.087	rigid zone
1639	8.26	0.037	rigid zone

of pH at the general structural level. Figure 6 shows the HPL spectra obtained at various pH levels in the 1750−1500 cm^{-1} range encompassing the amide I and II bands. The spectrum recorded at pH 6.5 was fitted by a deconvolution procedure using Gaussian functions. Deconvolution yielded a set of seven Gaussian functions for the amide I band, the centers, widths, and integrals of which are given in Table 1. The various peaks were attributed to various secondary structural elements (β-strands, α-helices, and turns) in line with previous studies (*21*). The peaks observed at 1630 and 1639 cm^{-1} corresponded to less than 2% of the total FTIR spectrum area and probably reflected highly rigid zones in the HPL. When only the β-strands and the α-helices were taken into account, the relative proportions obtained were 60 and 40%, respectively; these values are in agreement with previously published data on the X-ray crystallography structures (*3, 4*).

In the pH range of 4.0−6.5, the FTIR spectra obtained were superimposable (Figure 6) and stable with time (1 h), which indicates that the secondary structure of the HPL persisted. Conversely, the spectrum obtained at pH 2.5 was dramatically different from the others. A strong peak centered at 1620 cm^{-1}, which was that characteristic of an aggregated enzyme, appeared (*22*). This result shows that the overall structure of the protein is greatly modified at this pH value. In addition, the FTIR spectrum was found to evolve with time. The weak reproducibility of the measurements obtained at pH 2.5 made the deconvolution of the FTIR spectrum impossible.

DISCUSSION

The structural changes induced in HPL when the pH was lowered were studied here using an approach in which lipase adsorption and activity measurements were combined with SDSL-EPR and ATR-FTIR spectroscopic methods. The SDSL-EPR and ATR-FTIR experiments were performed in the absence of any physiological partners of HPL (such as lipids, bile salts, and colipase), the presence of which can affect the structure of HPL locally by inducing the opening of the lid and giving access to the active site (*6*), for example.

Within the pH range of 2.5−6.5, which includes the pH values naturally occurring in the gastrointestinal tract (*1, 13*−*15*), two pH domains were identified in which HPL undergoes various structural changes, with a threshold at a pH value of 3.0.

When HLP was incubated in solutions at pH values ranging from 4.0 to 6.5, it remained functionally stable for more than 2 h as shown by measuring its residual activity under optimized assay conditions (pH 7.5; Figure 2) and its ability to bind to a lipid−water interface (data not shown). The ATR-FTIR absorption spectra observed in the amide I band range showed that the secondary structure of HPL was globally unchanged, showing proportions of α-helices and β-sheets corresponding to those previously determined by X-ray crystallography (*3, 4*). These findings indicate that the α/β-fold in the N-terminal domain and the β-sandwich structure of the C-terminal domain of HPL are stable in this pH range or at least undergo only slight, reversible changes since the enzyme was found to be still active when its residual activity was tested at pH 7.5.

Below pH 3.0, HPL was rapidly inactivated (Figure 2) and the enzyme lost its ability to bind to lipid emulsions and colipase. The ATR-FTIR spectrum in the amine I band range shows that an irreversible change in the secondary structure of HPL takes place at pH 2.5, eventually leading to the aggregation of the enzyme.

SDSL-EPR spectroscopy was performed to examine more closely some of the local changes in the conformation of HPL that might be induced by pH variations. The EPR spectral shape of a spin-label grafted onto a protein side chain depends on its mobility and on the space available for it to wobble. This available space is governed by the internal dynamics of the spin-labeled side chain, by steric hindrance, and by fluctuations in the protein backbone (*23*). In this study, we have used the term "mobility" of the spin-label, which includes the mobility strictly speaking and the available space contributions, to describe the movement of spin-labels introduced into HPL. When the EPR spectra obtained are described, the "slow- and fast-motion components" always refer to the motion of the probe, although this motion can be affected by the motion of the 50 kDa HPL protein at a temperature of 25 °C. When the radical has a fast motion ($\tau \approx 10^{-9}$ s) in comparison with the rotational motion of HPL ($\tau \approx 10^{-8}$ s), the effects of the protein's motion on the overall motion of the radical can be neglected. When the motion of the radical slows, the slow-motion component of the EPR spectrum can be influenced by the motion of the protein. In any case, the changes observed in the EPR spectrum reflect motional changes that are mainly due to changes in the environment of the radical.

Since the nitroxide EPR spectra can be pH-sensitive and depend on the local polarity, the radical mobility might not be the only parameter which needs to be discussed in relation to the shape of the EPR spectra. We checked, however, that the EPR spectrum of MTSL was not sensitive to the pH (data not shown). The polarity of the radical environment can also change due to changes in the structure of the protein, and the hyperfine tensor component of the EPR spectrum can change accordingly. These changes can be expected to be quite small, however (in the range of a few Gauss), while those observed experimentally here (corresponding to an increase of 32 G between the outer peaks) are much larger and reflect a major contribution of the radical mobility to the overall mobility.

Nitroxide spin-labels were grafted either onto the lid (at position 249), which is known to undergo a local functional change in its conformation during catalysis by HPL, or at position 181 in a rigid part of HPL, based on the X-ray crystal structures. In addition to being easily accessible at the surface of the protein, position 181 is located in the same loop as the catalytic Asp176 residue, which is buried in the HPL core. At pH values ranging from 5.0 to 6.5, the EPR

spectral shapes of the spin-labels grafted onto both positions 181 and 249, and therefore their mobility, remained unchanged (Figure 3). These results mean that neither the steric hindrance exerted on the nitroxides, the backbone fluctuations, nor the internal dynamics of the side chains are affected under these conditions. These findings suggest that the structure of the lid and the structure of the protein in the vicinity of the catalytic aspartate are stable in this pH range.

At pH 4.0, the EPR spectral shapes of the spin-labels grafted at positions 249 and 181 indicated that their mobilities were modified in opposite ways (Figure 3A). An increasingly large proportion of the spin-labels grafted at position 249 became less mobile as the pH decreased to pH 4.0, whereas an increasingly large proportion of the spin-labels grafted onto position 181 became more mobile (Figure 3B). The slow-motion component of the EPR spectrum recorded with the spin-label at position 249 could be superimposed on that obtained with HPL in the presence of colipase and a micellar concentration of NaTDC (Figure 4). We previously reported that the lid exists in its open conformation under these conditions (*6*). These findings suggest that the HPL lid opens at pH 4.0 and that its open conformation is similar to that induced by NaTDC and colipase at pH 6.5 (Figure 4), since our EPR measurements indicate that under both of these experimental conditions, the label exhibits the same mobility. It is worth noting that the outer line splitting of this slow-motion component is equal to 6.6 mT, a value below the limit of 7.2 mT corresponding to an "immobilized" spin-label for EPR spectra recorded at X band. We were therefore still able to detect changes in mobility under these conditions. Moreover, since the FTIR-ATR measurements showed that the overall secondary structure of HPL is maintained at pH 4.0, the change in the mobility of the spin-label grafted onto the lid cannot be due to a large structural reorganization of the protein.

The changes in the mobility of the spin-label introduced at position 181 were not as large as those observed with the spin-label in the lid at pH 4.0. These findings are in good agreement with the crystallographic data, which have shown that the structure of HPL remains unchanged around this position when the lid opens (*3, 4*). In addition, similar results were previously obtained with HPL mixed with bile salts and colipase: the mobility of the spin-label grafted at this position was not found to be affected when the lid opening occurs in the presence of NaTDC and colipase. It is also worth noting that when HPL is present alone in solution, the opening of the HPL lid deduced from the changes in the spin-label mobility can already be detected at pH 5.0, whereas the increasing mobility observed with the spin-label grafted at position 181 only occurred at pH values much lower than 5.0. All in all, these results suggest that the increasing mobility of this spin-label does not result directly from the opening of the lid. It is merely due to a loss of tertiary contact of the side chain and/or an increasing level of backbone mobility around this position. Hence, some structural destabilization of HPL occurs in the vicinity of the catalytic aspartate (D176) at pH <5.0. It is worth noting, however, that all these structural changes were found to be reversible down to pH 3.0 (Figure 5).

A more pronounced destabilization of the HPL structure around position 181 was observed at pH <3.0. The EPR spectral shape observed at pH 2.5 indicates that the spin-label is highly mobile. These results suggest that HPL is unfolded around position 181, as previously observed with other proteins (*18*−*20*). The structural changes occurring at pH 2.5 were found to be irreversible.

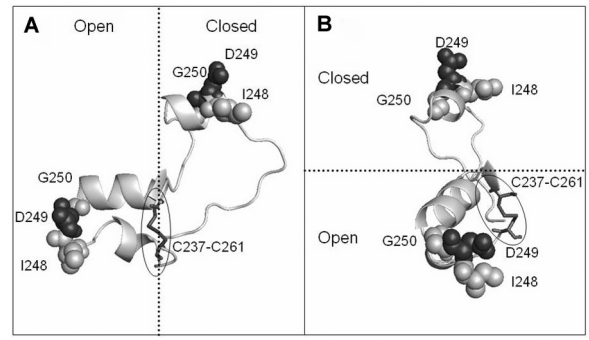

FIGURE 7: Open and closed conformations of the HPL lid showing the environment of residue D249. The peptide stretch C237−C261 is shown in the form of a ribbon model. The disulfide bridge between C237 and C261 is shown in the form of a stick model, whereas amino acid residues I248, D249, and G250 are shown in the form of CPK models. Panel B is the left side view corresponding to the view in panel A.

On the other hand, the large EPR spectral shape observed at pH 2.5 for the spin-label grafted onto the lid at position 249 was similar to that observed at pH 4.0, except that nearly all the molecules (90%) showed a low level of mobility. As the structure of the polypeptide chain undergoes a change in the vicinity of the catalytic aspartate, and as the overall secondary structure of HPL is also modified, the lid is probably exposed to an environment very different from that occurring at higher pH values and when HPL is stable. However, since the slow-motion EPR spectrum component of the spin-label grafted onto the lid was found to be identical to that observed with both the open and folded HPL, the lid seems to preserve its local structure at pH 2.5, although HPL is completely unfolded, as shown by the FTIR data. In this case, the conformation of the lid observed in the open form of HPL is probably more stable than that observed in the closed form of HPL. The latter conformation might be stabilized by the intramolecular interactions with the protein core and the β5 loop observed in the crystal structure of the protein (*24*). Figure 7 shows the location of residue 249 within the HPL lid. In the closed conformation, D249 is located in the short, single α-helix of the lid. In the open conformation, the secondary structure of the lid changes drastically and D249 is now to be found in a loop forming an elbow between two α-helices connected by the disulfide bridge (C237−C261). In both situations, the side chain of D249 is still accessible to solvent [which is the reason why this residue was selected here (*6*)], but the environment of the D249 side chain seems to be more strictly constrained in the open conformation due to the presence of neighboring side chains and the rigidity introduced by the two α-helices and the disulfide bridge. This might explain why the spin-label is less mobile under these conditions, although it is usually reported that exposed spin-labels in α-helices are less mobile than those present in loops (*25*).

All our findings on the structural and functional effects of the pH on HPL indicate that pH 3.0 is a critical value. Above this value, the secondary structure of this enzyme is conserved, and the structural changes observed in the vicinity of the catalytic site (such as the opening of the lid, the

decreasing steric hindrance, and/or the increasingly large backbone fluctuations near the catalytic D176) are reversible. Below pH 2.5, an irreversible structural change takes place: the overall secondary structure is modified, and the protein aggregates. HPL therefore no longer binds to lipid emulsions, and its activity is not recovered when the pH is shifted back to neutral levels.

A good correlation exists between these results and the HPL stability observed for these pH ranges. It was not possible, however, to establish a correlation between the EPR data (reversible) and the enzyme stability (slow and irreversible inactivation with time) at the particular pH value of 3.0.

The local structural stability of HPL was investigated around only two positions, which are located near the active site. It is possible that a pH-dependent structural destabilization of HPL may also occur in other regions of this protein, but any such structural changes will obviously be reversible at pH >3.0, since after incubation in this pH range, the functional properties of HPL tested at the optimum pH of 7.5 were found to be preserved.

Since the opening of the HPL lid seems to be pH-dependent and reversible at pH >3.0, this conformational change might result from changes in the electrostatic interactions stabilizing either the closed or the open conformation of the lid. Several salt bridges have been identified in the crystal structures of the closed and open HPL. When the lid was in the open conformation, two salt bridges between residues D79 (β5 loop) and R256 (lid) and between residues D257 (lid) and K268 (protein core) were observed, as well as a hydrogen bond between residues E83 (β5 loop) and W252 (lid) (*4*). When the lid was in the closed conformation, residue D79 (in the β5 loop) was also found to be involved in an interaction between the β5 loop and the lid. In the closed conformation, the β5 loop makes contact exclusively with the closed lid (*4*). Without this support, it was suggested that this loop might fold back upon the core of the protein (*4*), and this is actually what was observed in the open HPL (*4*), as well as in a pancreatic lipase having no lid (*26*), where the β5 loop adopts a conformation creating a functional oxyanion hole. Since the main opening of the lid occurs between pH 5.0 and 4.0 and is not accompanied by any other major change in the overall HPL structure, it seems likely that some interactions might be lost due the protonation of acidic residues. In line with this hypothesis, the lid might open because the closed conformation is no longer stabilized by electrostatic interactions, and this would suggest once again that the open conformation of the lid is more stable than the closed one.

When the lid opening process was previously observed at pH 6.5 in the presence of bile salts and colipase, it was suggested that the open conformation of the HPL was stabilized by hydrophobic interactions occurring on the apolar side of the lid with bile salt molecules and that the low mobility shown by the spin-label at position 249 probably resulted from this interaction (*6*). Since the same EPR spectrum was obtained here at low pH levels without the presence of bile salts, we can now rule out this hypothesis. The low mobility of the spin-label observed at position 249 is therefore merely due to an intrinsic structural reorganization of the lid associated with the opening process, as discussed above in connection with Figure 7.

In conclusion, this study shows that a parameter such as the pH can affect the structure of pancreatic lipase in various ways, in a manner independent of other parameters such as the presence of lipids and amphiphiles. These modifications range from a local conformational change in the lid giving access to the active site to the complete unfolding and aggregation of the protein. From the kinetic point of view, the effects of pH on the opening of the lid can be compared with the effects of pH on the other important steps in the process of interfacial catalysis (Figure 1). The pH is known to affect the rate of lipase adsorption at the lipid interface significantly, and not only the formation of the enzyme−substrate complex followed by the process of hydrolysis (*10*). These results show that the conformational changes occurring during this type of catalytic event can also be pH-dependent. This means that when the effects of pH on enzyme activity are studied, the profile obtained reflects a combination of at least these three steps. We can therefore forget about the classical hypothesis according to which the ascending part of a pH-dependent activity curve reflects the state of ionization of the catalytic histidine residue in enzymes with a Ser-His-Asp triad.

Studying the effects of pH on pancreatic lipase over a large pH range is also relevant from a physiological point of view. HPL is normally exposed in vivo to pH values ranging from 5.5 to 6.5 on average (*1, 12, 13*), but pH values as low as 2.0−3.0 can be observed in the duodenal contents of patients with EPI (*14, 15*). This acidification of duodenal contents during digestion of meals is due to the fact that gastric acid is no more neutralized by pancreatic bicarbonate which is also missing in EPI. Thus, the HPL naturally present in the residual secretion of the exocrine pancreas or pancreatic lipase given orally to patients with EPI will face sometimes very low pH values at specific sites of the gastrointestinal tract. Understanding effects of pH on pancreatic lipase at the molecular level might therefore be useful for improving enzyme stability and activity for the treatment of EPI.

ACKNOWLEDGMENT

We thank Dr. Robert Verger for fruitful discussions and his continuous interest in this work. We are grateful to Camille Mascle Allemand and Jean-Pierre Duneau (CNRS, UPR 9027, Marseille, France) for their technical support with the ATR-FTIR spectroscopy and to Dr. Jessica Blanc for revising the English manuscript.

REFERENCES

1. Carrière, F., Barrowman, J. A., Verger, R., and Laugier, R. (1993) Secretion and contribution to lipolysis of gastric and pancreatic lipases during a test meal in humans. *Gastroenterology 105*, 876–888.
2. Winkler, F. K., d'Arcy, A., and Hunziker, W. (1990) Structure of human pancreatic lipase. *Nature 343*, 771–774.
3. van Tilbeurgh, H., Sarda, L., Verger, R., and Cambillau, C. (1992) Structure of the pancreatic lipase-procolipase complex. *Nature 359*, 159–162.
4. van Tilbeurgh, H., Egloff, M.-P., Martinez, C., Rugani, N., Verger, R., and Cambillau, C. (1993) Interfacial activation of the lipase-

procolipase complex by mixed micelles revealed by X-ray crystallography. *Nature 362*, 814–820.
5. Chahinian, H., Bezzine, S., Ferrato, F., Ivanova, M. G., Perez, B., Lowe, M. E., and Carriere, F. (2002) The $\beta 5'$ loop of the pancreatic lipase C2-like domain plays a critical role in the lipase-lipid interactions. *Biochemistry 41*, 13725–13735.
6. Belle, V., Fournel, A., Woudstra, M., Ranaldi, S., Prieri, F., Thome, V., Currault, J., Verger, R., Guigliarelli, B., and Carriere, F. (2007) Probing the Opening of the Pancreatic Lipase Lid Using Site-Directed Spin Labeling and EPR Spectroscopy. *Biochemistry 46*, 2205–2214.
7. Cajal, Y., Svendsen, A., Girona, V., Patkar, S. A., and Alsina, M. A. (2000) Interfacial control of lid opening in *Thermomyces lanuginosa* lipase. *Biochemistry 39*, 413–423.
8. Carrière, F., Moreau, H., Raphel, V., Laugier, R., Bénicourt, C., Junien, J.-L., and Verger, R. (1991) Purification and biochemical characterization of dog gastric lipase. *Eur. J. Biochem. 202*, 75–83.
9. Roussel, A., Miled, N., Berti-Dupuis, L., Riviere, M., Spinelli, S., Berna, P., Gruber, V., Verger, R., and Cambillau, C. (2002) Crystal structure of the open form of dog gastric lipase in complex with a phosphonate inhibitor. *J. Biol. Chem. 277*, 2266–2274.
10. Chahinian, H., Snabe, T., Attias, C., Fojan, P., Petersen, S. B., and Carrière, F. (2006) How gastric lipase, an interfacial enzyme with a Ser-His-Asp catalytic triad, acts optimally at acidic pH. *Biochemistry 45*, 993–1001.
11. Borgström, B. (1975) On the interactions between pancreatic lipase and colipase and the substrate, and the importance of bile salts. *J. Lipid Res. 16*, 411–417.
12. Carriere, F., Renou, C., Ransac, S., Lopez, V., De Caro, J., Ferrato, F., De Caro, A., Fleury, A., Sanwald-Ducray, P., Lengsfeld, H., Beglinger, C., Hadvary, P., Verger, R., and Laugier, R. (2001) Inhibition of gastrointestinal lipolysis by Orlistat during digestion of test meals in healthy volunteers. *Am. J. Physiol. 281*, G16−G28.
13. Lengsfeld, H., Beaumier-Gallon, G., Chahinian, H., De Caro, A., Verger, R., Laugier, R., and Carrière, F. (2004) Physiology of gastrointestinal lipolysis and therapeutical use of lipases and digestive lipase inhibitors. In *Lipases and phospholipases in drug development* (Müller, G., and Petry, S., Eds.) pp 195−229, Wiley-VCH, Weinheim, Germany.
14. Carriere, F., Grandval, P., Renou, C., Palomba, A., Prieri, F., Giallo, J., Henniges, F., Sander-Struckmeier, S., and Laugier, R. (2005) Quantitative study of digestive enzyme secretion and gastrointestinal lipolysis in chronic pancreatitis. *Clin. Gastroenterol. Hepatol. 3*, 28–38.
15. Barraclough, M., and Taylor, C. J. (1996) Twenty-four hour ambulatory gastric and duodenal pH profiles in cystic fibrosis: Effect of duodenal hyperacidity on pancreatic enzyme function and fat absorption. *J. Pediatr. Gastroenterol. Nutr. 23*, 45–50.
16. Thirstrup, K., Carrière, F., Hjorth, S., Rasmussen, P. B., Wöldike, H., Nielsen, P. F., and Thim, L. (1993) One-step purification and characterization of human pancreatic lipase expressed in insect cells. *FEBS Lett. 327*, 79–84.
17. Bezzine, S., Ferrato, F., Ivanova, M. G., Lopez, V., Verger, R., and Carriere, F. (1999) Human pancreatic lipase: Colipase dependence and interfacial binding of lid domain mutants. *Biochemistry 38*, 5499–5510.
18. Columbus, L., and Hubbell, W. L. (2004) Mapping backbone dynamics in solution with site-directed spin labeling: GCN4-58 bZip free and bound to DNA. *Biochemistry 43*, 7273–7287.
19. Morin, B., Bourhis, J. M., Belle, V., Woudstra, M., Carriere, F., Guigliarelli, B., Fournel, A., and Longhi, S. (2006) Assessing induced folding of an intrinsically disordered protein by site-directed spin-labeling electron paramagnetic resonance spectroscopy. *J. Phys. Chem. B 110*, 20596–20608.
20. Belle, V., Rouger, S., Costanzo, S., Liquiere, E., Strancar, J., Guigliarelli, B., Fournel, A., and Longhi, S. (2008) Mapping α-helical induced folding within the intrinsically disordered C-terminal domain of the measles virus nucleoprotein by site-directed spin-labeling EPR spectroscopy. *Proteins 73*, 973–988.
21. Barth, A. (2007) Infrared spectroscopy of proteins. *Biochim. Biophys. Acta 1767*, 1073–1101.
22. Natalello, A., Ami, D., Brocca, S., Lotti, M., and Doglia, S. M. (2005) Secondary structure, conformational stability and glycosylation of a recombinant *Candida rugosa* lipase studied by Fourier-transform infrared spectroscopy. *Biochem. J. 385*, 511–517.
23. Columbus, L., and Hubbell, W. L. (2002) A new spin on protein dynamics. *Trends Biochem. Sci. 27*, 288–295.
24. Carrière, F., Thirstrup, K., Boel, E., Verger, R., and Thim, L. (1994) Structure-function relationships in naturally occurring mutants of pancreatic lipase. *Protein Eng. 7*, 563–569.
25. Mchaourab, H. S., Lietzow, M. A., Hideg, K., and Hubbell, W. L. (1996) Motion of spin-labeled side chains in T4 lysozyme. Correlation with protein structure and dynamics. *Biochemistry 35*, 7692–7704.
26. Withers-Martinez, C., Carrière, F., Verger, R., Bourgeois, D., and Cambillau, C. (1996) A pancreatic lipase with a phospholipase A1 activity: Crystal structure of a chimeric pancreatic lipase-related protein 2 from guinea pig. *Structure 4*, 1363–1374.

BI801250S